Review

MOLECULAR METABOLISM

$Na_V1.8$ neurons are involved in limiting acute phase responses to dietary fat

Swalpa Udit [1], Michael Burton [1], Joseph M. Rutkowski [2], Syann Lee [1], Angie L. Bookout [1,3], Philipp E. Scherer [2], Joel K. Elmquist [1,**], Laurent Gautron [1,*]

ABSTRACT

Objective and methods: Metabolic viscera and their vasculature are richly innervated by peripheral sensory neurons. Here, we examined the metabolic and inflammatory profiles of mice with selective ablation of all $Na_V1.8$-expressing primary afferent neurons.

Results: While mice lacking sensory neurons displayed no differences in body weight, food intake, energy expenditure, or body composition compared to controls on chow diet, ablated mice developed an exaggerated inflammatory response to high-fat feeding characterized by bouts of weight loss, splenomegaly, elevated circulating interleukin-6 and hepatic serum amyloid A expression. This phenotype appeared to be directly mediated by the ingestion of saturated lipids.

Conclusions: These data demonstrate that the $Na_V1.8$-expressing afferent neurons are not essential for energy balance but are required for limiting the acute phase response caused by an obesogenic diet.

Keywords Deafferentation; Diphtheria toxin; Energy homeostasis; Nodose ganglion; Inflammation; Obesity

1. INTRODUCTION

Obesity is closely linked with low-grade inflammation, characterized by increased levels of circulating inflammatory cytokines and acute-phase reactants, concomitant with the activation of inflammatory signaling pathways [1,2]. In particular, interleukin-6 circulates at higher levels than other pro-inflammatory cytokines in human obesity and is tightly correlated with the degree of adiposity [3–6]. This obesity-dependent inflammation differs from other inflammatory paradigms in its association with chronic activation of the innate immune system and its multi-organ involvement [1,7]. Epidemiological, clinical, and experimental evidence causally links this inflammatory state to the development of comorbidities that emerge from obesity, including insulin resistance, type 2 diabetes, fatty liver disease, atherosclerosis, dementia, respiratory diseases, and cancers [1,2]. While it is well-appreciated that nutrient excess from carbohydrate-rich and fatty foods induces a characteristic inflammatory response [8], much of how diet-induced inflammation is regulated at the organismal level remains to be understood.

The physiological state of much of the body is monitored by a system of neurons including small-diameter, primary afferent neurons that convey information from virtually all visceral tissues and, ultimately, guide the physiological processes necessary to maintain homeostasis [9]. Among these afferent neurons are populations of vagal and spinal sensory neurons that express the receptors necessary to rapidly respond to food-related stimuli, injuries, and changes in local metabolism [10–14]. Afferent neurons in the vagal and spinal nerves, therefore, may serve as a critical link between dietary nutrient sensing and the coordinated control of the various physiological responses to diet-induced obesity.

To test the role of primary afferent neurons in coordinating responses to excess caloric intake, we utilized a previously described genetic mouse model of primary afferent neuron ablation by crossing two mouse lines, floxed-Stop-DTA and $Na_V1.8$-Cre mice. Floxed-Stop-DTA mice express diphtheria toxin subunit A (DTA) after the Cre-mediated, cell-type-specific removal of a transcriptional blocker [15]. The $Na_V1.8$ knock-in Cre mouse expresses Cre-recombinase under the control of the $Na_V1.8$ promoter [16], a tetrodotoxin-resistant, voltage-gated sodium channel previously implicated in the genesis of action potentials in nociceptors [17]. $Na_V1.8$-expressing neurons correspond to small-diameter dorsal root ganglion (DRG) neurons [16,18,19] and approximately 80% of vagal afferent neurons in the nodose ganglion (NG) [16,20,21], including neurons connected to the gastrointestinal tract. Therefore, $Na_V1.8$-Cre mice are ideal for targeting large subsets of both vagal and spinal afferent neurons that are thought to be concerned with nutrient sensing and that innervate key endocrine and metabolic tissues [20]. Mice carrying one copy of $Na_V1.8$-Cre and one floxed-Stop-DTA allele were generated, resulting in the irreversible ablation of all $Na_V1.8$-expressing neurons, and systematically compared to $Na_V1.8$-Cre

[1]Division of Hypothalamic Research, Department of Internal Medicine, The University of Texas Southwestern Medical Center, 5323 Harry Hines Blvd., Dallas 75390, TX, USA [2]Touchstone Diabetes Center, Department of Internal Medicine, The University of Texas Southwestern Medical Center, 5323 Harry Hines Blvd., Dallas 75390, TX, USA [3]Department of Pharmacology, The University of Texas Southwestern Medical Center, 5323 Harry Hines Blvd., Dallas 75390, TX, USA

*Corresponding author. E-mail: Laurent.Gautron@UTSouthwestern.edu (L. Gautron).

**Corresponding author. E-mail: Joel.Elmquist@utsouthwestern.edu (J.K. Elmquist).

Received July 6, 2017 • Revision received July 19, 2017 • Accepted July 24, 2017 • Available online 4 August 2017

http://dx.doi.org/10.1016/j.molmet.2017.07.012

littermates with intact neurons. This ablation model has been previously used [15] to demonstrate that $Na_v1.8$-expressing spinal sensory neurons mediate sensing of cold as well as inflammatory and mechanical pain, but the role of these neurons in response to metabolic challenges has never been investigated.

2. MATERIALS AND METHODS

2.1. Mice and breeding strategy

$Na_v1.8$ knock-in Cre-recombinase mice on a pure C57Bl/6J background were obtained from Dr. John Wood (University College London) [16]. The $Na_v1.8$-Cre fragment or wild-type band was detected by PCR with the following primers: a) 5′-TGTAGATGGACTGCAGAGGATGGA-3′ (common forward); b) 5′-TTACCCGGTGTGTGCTGTAGAAAG (reverse wild-type); c) 5′-AAATGTTGCTGGATAGTTTTTACTGCC-3′ (reverse Cre). Importantly, $Na_v1.8$-Cre mice show no Cre activity outside of the peripheral nervous system during development or adulthood [16,20]. Furthermore, we also verified by biochemical and histological means that exposure to high-fat diet did not induce ectopic Cre-recombinase activity in peripheral tissues. Finally, the initial characterization of the mice demonstrated that the introduction of the Cre-recombinase did not affect metabolism and that mice with only one $Na_v1.8$-Cre allele showed no metabolic anomalies (glucose level, body length, body weight and composition, or weekly food intake) on chow or high-fat diet (not shown). Heterozygous $Na_v1.8$-Cre mice were crossed with homozygous ROSA26-eGFP-DTA mice (stock #006331; The Jackson Laboratory, USA) to generate litters with a 1:1 ratio of littermate controls and ablated mice. Genomic DNA was isolated from the tail. The DTA wild-type fragment and floxed fragment were detected by PCR with the following primers: a) 5′- AAAGTCGCTCTGAGTTGTTAT-3′ (common forward); b) 5′-GGAGCGGGAGAAATGGATATG-3′ (reverse wild-type); c) 5′- GCGAAGAGTTTGTCCTCAACC-3′ (reverse DTA). Ablated mice consisted of males carrying one Cre allele and one DTA allele. Control littermates carried only one Cre allele. Mice were all housed in a light-controlled (12 h on/12 h off; lights on at 6 AM) and temperature-controlled environment (21.5—22.5 °C) within a barrier facility. Mice were fed chow or a high-fat diet, providing 12% or 42% energy percent as triglycerides (2016 or TD.88137, Harlan Teklad), respectively. The high-fat diet was 42% Kcal from milkfat fat with saturated fat representing 12.8% of the diet. Monounsaturated and polyunsaturated fat represented 5.6% and 1% of the diet, respectively. The animals and procedures used were approved by the Institutional Animal Care and Use Committee at the University of Texas Southwestern Medical Center at Dallas.

2.2. Histology

For *in situ* hybridization, mice were anesthetized using an intraperitoneal i.p. injection of chloral hydrate (350 mg/kg) and then perfused transcardially with DEPC-treated 0.9% saline followed by 10% neutral buffered formalin. NG and DRG were removed, equilibrated overnight with 20% sucrose solution, and cryostat-cut at 16 μm thickness into five equal series. *In situ* hybridization for $Na_v1.8$ mRNA was performed as previously described using the same antisense S^{35}-labeled riboprobe and protocol [22]. No signals were detected using the sense probe [22]. *In situ* hybridization was performed in a total of three ablated and three control young males.

For isolectin B4 binding, fixed ganglia were incubated overnight at room temperature with biotinylated-IB4 (Sigma; 5 mg/ml), followed by 1 h of AlexaFluor 594-conjugated streptavidin (Life Technologies; cat#S32356). Isolectin B4 binding was assessed on the ganglia of three ablated and three control young males.

For hematoxylin and eosin staining, mice were perfused transcardially with 0.9% saline followed by 10% neutral buffered formalin. Spleens were then collected and stored in 50% ethanol. Hematoxylin and eosin staining was subsequently performed in paraffin-embedded samples using standard protocols by the UT Southwestern Histology Core. Staining was performed in a total of three ablated and three control males fed on high-fat diet for 9 weeks.

For immunohistochemistry, mice were perfused transcardially with 0.9% saline followed by 10% neutral buffered formalin as described above. Tissues were post-fixed for 1 h and incubated overnight in a solution of 20% sucrose. Nodose ganglia and spleens were next cryostat-cut at 16 μm into five equal series. Brainstems were cut using a freezing microtome (Leica) at 25 μm thickness into five equal series. Immunohistochemistry was performed using antisera against c-Fos (Santa Cruz; cat#sc-52, rabbit polyclonal), with 3% normal donkey serum (NDS; Jackson ImmunoResearch) and 0.3% Triton X-100 in phosphate-buffered saline (PBS) at room temperature. CD3 and CD19 antisera were followed by secondary AlexaFluor 594-conjugated anti-rabbit (Invitrogen; cat#A21207), or anti-mouse (Invitrogen; cat#A11001). The c-Fos primary was followed by a biotinylated anti-rabbit antibody (Jackson ImmunoResearch; cat#711-065-152) and the Vectastain ABC kit. Revelation for c-Fos was achieved using a mixture of 0.04% DAB, 0.01% H_2O_2, 0.02% nickel sulfate, and 0.02% cobalt chloride. Images were captured using the brightfield or epifluorescence optics of a Zeiss microscope (Imager Zl) attached to a digital camera (AxioCam). Fos immunohistochemistry was performed on the brainstem of six ablated and seven controls, fed a large fatty meal, respectively.

2.3. Real-time PCR analysis

Total RNA was isolated from NG with the Ambion® RiboPure Kit (Invitrogen) and from all other issues with RNA Stat-60 (Tel Test, Inc.) in accordance with the manufacturers' instructions. The DNA in the samples was removed with RNase-Free DNase (Invitrogen). Complementary DNA (cDNA) was generated from 2 μg of RNA with the High Capacity cDNA Reverse Transcription Kit (Applied Biosystems) for most tissues. For NG samples, cDNA was generated from 8 ng of RNA with High Capacity cDNA Reverse Transcription Kit (Applied Biosystems); then, cDNA was pre-amplified using the TaqMan® PreAmp Master Mix (Applied Biosystems). QPCR was then performed with SYBR GreenER™ qPCR SuperMix (Applied Biosystems). Pre-validated Taqman assays were used (5′-FAM; Applied Biosystems) according to published protocols [23]. Levels were normalized to levels of ribosomal RNA 18S. All assays were performed using an Applied Biosystems Prism 7900HT sequence detection system. The sequence of our primers is available upon request.

2.4. Temperature measurement

TA-F10 telemeters (Data Science International, St Paul, MN) were intraperitoneally implanted in anesthetized (ketamine/xylazine) mice. After allowing a week for recovery, we continuously recorded body temperature in mice that were fed *ad libitum* on chow, then subjected to an overnight fast, and subsequently switched to a high-fat diet (42%). Ambient temperature was maintained at approximately 23 °C.

2.5. Metabolic chambers

Body weight-matched mice of 12 weeks of age were used for indirect calorimetry studies (LabMaster Calorimetry System, TSE Systems; University of Texas Southwestern Mouse Metabolic Phenotyping Core). Measurements were performed after a 5-d acclimation in home cages with *ad libitum* access to food and water. Room temperature was

maintained at 22 °C with a 12-h light/dark cycle. O_2 consumption and CO_2 production were measured for 5 d after acclimation. These values were normalized (calculated as body weight to the 0.75 power). During this time, ambulatory and rearing activities were also monitored with infrared beams. In addition, meal patterns were determined temporally integrating data from weigh sensors fixed at the top of the cage; the food containers were suspended from these sensors into the sealed cage environment. Meals were defined as food intake events with a minimum duration of 60 s, and a break of 300 s between food intake events. To assess the metabolic responses to a high fat diet, mice were acclimatized in the TSE metabolic chambers as described above. Food was switched from chow to the high-fat diet at 17:00 on day 3, and metabolic parameters were continuously monitored for the following 2 d.

2.6. Chronic high-fat feeding

Control and ablated mice were switched to a high-fat diet (42% as described before) starting at 6 weeks of age. Their body weight was measured on a weekly basis for 9 weeks. On the day of sacrifice, spleen weight was measured in subsets of high-fat fed mice. Blood was collected by cardiac puncture in EDTA tubes. The samples were then spun at 3000 rcf for 20 min at 4 °C, and plasma was stored at −80 °C until measurement assays were conducted. Cytokines were measured using the Luminex® Multiplex System in the University of Texas Southwestern Mouse Metabolic Phenotyping Core. In parallel, liver samples were rapidly frozen in liquid nitrogen for qPCR assays.

2.7. Refeeding experiment

Activation of the dorsovagal complex in response to a large meal was assessed using a protocol adapted from [24]. Briefly, over 5 consecutive days, ablated and control mice were given access high-fat diet (42%) for 1 h each morning (9—10 AM) and chow for 3 h each afternoon (3—6 PM). On the last day, mice were transcardiacally perfused 1 h 30 min after being given access to a high-fat diet. Their stomachs were also weighed at the time of sacrifice.

2.8. Lard oil gavage

Four hours before the gavage, mice were singly housed without food. Immediately prior to gavaging, blood was collected via tail bleed in EDTA tubes. At time 0, mice were gavaged with 10 μl/g lard oil (Sigma). Blood was collected at 30 min and 1, 2, 3, 4, 5, and 6 h post-gavage and kept on ice. The samples were then centrifuged at 3000 rcf for 5 min. Levels of plasma triglycerides and non-esterified fatty acids were measured per manufacturer's instructions using the Infinity Triglycerides kit (Fisher) and the HR Series NEFA-HR(2) kit (Wako Diagnostics), respectively. Separate cohorts of ablated and control mice were gavaged with lard oil or 0.9% sterile saline. Three hours later, their blood and liver were collected.

2.9. Statistical analysis

All values are presented as the means ± SEM. Animal numbers are indicated in the figure legends. Data were analyzed with Student's t test and one-way or two-way ANOVA. Correction for multiple comparisons was performed as recommended by GraphPad Prism 7.01. Differences were considered significant at $p < 0.05$.

3. RESULTS

3.1. Validation of ablation of $Na_v1.8$ neurons

The ablation of vagal and spinal $Na_v1.8$-expressing neurons was validated using histological and biochemical experiments. In situ hybridization for $Na_v1.8$ mRNA in NG and DRG showed that no $Na_v1.8$-expressing neurons were retained in ablated mice (Figure 1A—D). The sensory ganglia of ablated mice were visibly smaller (Figure 1B and D), and immunostaining studies further confirmed the complete ablation of neurons marked by IsB4 binding (a marker for C-fibers) (Figure 1E and F). In contrast, innervation by motor autonomic and enteric neurons remained intact in ablated mice, as shown by our immunostaining studies (Figure S1). Ablation of $Na_v1.8$ neurons was further assessed using quantitative real-time PCR (QPCR) studies. QPCR revealed an almost complete loss of expression of three voltage-gated Na+ channels present in $Na_v1.8$ neurons including $Na_v1.8$ itself, $Na_v1.9$ and $Na_v1.7$ (Table 1). Likewise, expression of several channels and receptors known to be enriched in C-fibers was eliminated or significantly reduced in the nodose ganglion of ablated mice (Table 1). In contrast, genes preferentially expressed in A-fibers were only partially or non-significantly reduced in ablated animals (Table 1).

3.2. $Na_v1.8$ neurons are dispensable to the regulation of energy balance

Before entering metabolic cages, 12-week-old ablated mice fed on standard chow diet (4%) showed no difference in body weight or composition compared to ablated mice (Figure 2A). Food intake was not significantly different in ablated and control mice either when fed on chow or when switched to the high-fat diet (42%) (Figure 2B). On both diets, respiratory exchange ratio and parameters related to metabolic rate including oxygen consumption were identical in ablated mice and control littermates (Figure 2C and D). Ablated mice showed normal ambulatory movements when fed on chow (Figure 2E). In response to the high-fat diet, ablated animals showed a non-significant trend toward reduced locomotor activity (Figure 2E). Lastly, core body temperature was assessed in a separate cohort of ablated and control mice. Ablated mice showed no obvious thermoregulatory defects either under basal conditions or in response to fasting or high-fat feeding (Figure 2F).

Meal patterns were also assessed in the metabolic chambers. Overall, meal parameters were identical in ablated and control mice fed on chow (Figure 3A—F). When switched to the high-fat diet, both groups of mice modified their total number of meals and intermeal intervals in a similar fashion (Figure 3B and E). Nonetheless, we noticed subtle anomalies in the responses of ablated mice to the high-fat diet. Unlike control mice, ablated mice did not adjust their feeding rate and meal size (Figure 3A,C,D). Due to compensatory adjustments in other parameters, daily food intake remained identical in both experimental groups and dietary regimens (Figure 3F).

In support of minimally altered meal regulation in ablated mice, c-Fos immunoreactivity in the dorsovagal complex induced by a large fatty meal was identical of both groups of animals (Figure 3G and H). Moreover, the number of c-Fos-positive cells in the nucleus of the solitary tract of controls and ablated mice correlated well with their stomach weight rather than genotype (Figure 3I).

3.3. Lack of $Na_v1.8$ neurons exacerbates dietary fat-induced acute phase response

The metabolic screening of diet-induced obesity in ablated mice was complicated by the fact that ablated mice gradually started to show several physiological, biochemical, and histological anomalies that were never seen in chow-fed animals. Specifically, when chronically fed on the high-fat diet, individual ablated mice exhibited bouts of pronounced weight loss after a variable period of initial weight gain (Figure 4A). Indeed, their weight gain curve was only skewed toward the lowest values. When the data were individually plotted as weekly body change,

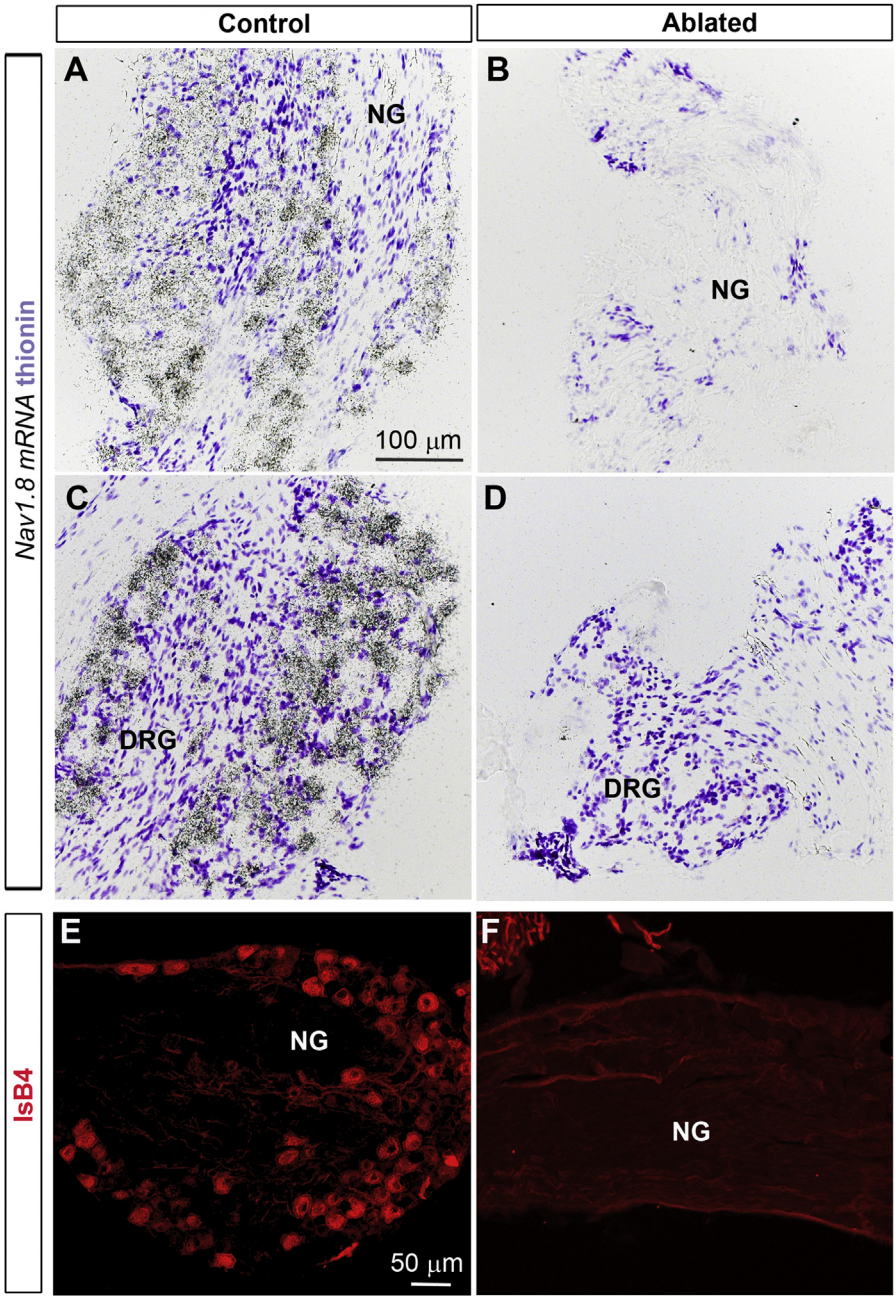

Figure 1: Ablation of vagal and spinal $Na_v1.8$-expressing neurons using conditional expression of diphtheria toxin. (**A**—**D**) *In situ* hybridization of NG and DRG with $Na_v1.8$ antisense riboprobe in control and ablated mice. $Na_v1.8$ mRNA signals represented by silver grains can be seen in many neurons of the NG and DRG of control mice, but not at all in ablated mice. Note also that sensory ganglia appear visibly smaller in ablated animals. (**E**—**F**) Isolectin B4 (IsB4) binding is commonly used as a surface marker of non-peptidergic C-fibers. No IsB4-positive cell bodies were retained in ablated mice, thus confirming the absence of C-fiber neurons.

it became apparent that about 1/3 of ablated mice showed sudden and transient weight loss after a variable period of initial weight gain (Figure 4A). The rest of the ablated animals gained the same amount of weight as control littermates. This loss of body weight did not present with overt signs of illness. However, necropsy of ablated mice on high-fat diet consistently revealed splenomegaly (Figure 4B). Splenomegaly was further confirmed by histology with enlarged red pulp and leucopenia in the white pulp (Figure 4C). Moreover, circulating interleukin-6 (IL-6), but not other pro-inflammatory cytokines, was elevated in high-fat fed ablated mice (Figure 4D). Lastly, ablated mice on the high-fat diet showed a robust induction of hepatic serum amyloid A (SAA1) mRNA, thus implying an acute phase inflammatory response (Figure 4E). However, no apparent foci of infection (e.g., bacterial translocation) or other cause of decline (e.g., portal hypertension) could be identified by pathologic or histopathologic examination. High-fat feeding similarly raised immunoglobulins against lipopolysaccharides in ablated and control mice (Figure S2A), suggesting identical intestinal permeability to bacterial endotoxins. The lack of $Na_v1.8$ neurons did not affect intestinal permeability to fluorescein isothiocyanate-conjugated dextran (Figure S2A).

The literature suggests a strong relationship between dietary saturated lipids, IL-6, and hepatic SAA1 [3—6]. Hence, to gain insight into the

Table 1 — Validation of ablation of vagal C-fibers using qPCR. Gene expression for varied receptors and channels was compared in the NG of ablated and control mice.

Gene of Interest	Fold Change	SEM	p-value	Known cell Function(s)
C-fiber enriched channels and receptors				
$Na_v1.8$	0.01	< 0.01	**0.0005**	Electrogenesis
$Na_v1.9$	0.02	0.01	**0.0006**	Electrogenesis
$Na_v1.7$	0.18	0.06	**0.0028**	Electrogenesis
HTR-3A	0.06	0.02	**0.0013**	Serotonin signaling
TRPV1	0.04	0.01	**< 0.0001**	Heat/capsaicin sensing
TRPA1	0.04	0.02	**0.0001**	Cold, stretch, irritants sensing
TRPC3	0.11	0.08	**0.0355**	Mechanoreceptor
P2X3R	0.20	0.05	**0.0027**	ATP/inflammation sensing
A-fiber enriched channels and receptors				
$Na_v1.1$	0.39	0.15	**0.0146**	Electrogenesis
$Na_v1.6$	0.52	0.19	**0.0443**	Electrogenesis
TRPM8	0.65	0.18	0.1533	Cold sensor
ATR-1A	0.41	0.09	0.1743	Angiotensin signaling

p-Values <0.05 indicated in bold (statistically significant). A fold change ≤ 0.2 is considered the arbitrary cut-off between complete (red) versus partial reduction (blue) in gene expression.

Abbreviations: ATR-1A, angiotensin receptor 1A; HTR-3A, 5-hydroxytryptamine receptor 3A; $Na_v1.1$, sodium channel, voltage-gated, type I, alpha subunit (SCN1A); $Na_v1.6$, sodium channel, voltage gated, type VIII, alpha subunit (SCN8A); $Na_v1.7$, sodium voltage-gated channel alpha subunit 9 (SCN9A); $Na_v1.8$, sodium voltage-gated channel alpha subunit 10 (SCN10A); $Na_v1.9$, sodium channel, voltage-gated, type XI, alpha subunit (SCN11A); P2X3R, purinergic receptor P2X3; TRPA1, Transient receptor potential cation channel, subfamily A, member 1; TRPC3, Short transient receptor potential channel 3; TRPM8, Transient receptor potential cation channel subfamily M member 8; TRPV1, transient receptor potential cation channel subfamily V member 1.

cause of this diet-induced inflammatory phenotype and rule out opportunistic infections, mice were studied after the acute gavage of lard oil. A primary alteration in lipid absorption was ruled out, as the kinetics of triglyceride appearance in the blood stream was equivalent between the two groups after gavages of saturated fatty acid (Figure 5A and B). However, lard oil triggered profound elevation in hepatic SAA1 mRNA that was not observed in the control littermates (Figure 5C). Plasma IL-6 was also significantly more elevated in ablated mice receiving lard oil (Figure 5D).

4. DISCUSSION

Intact vagal and spinal afferent neurons are required for the regulation of systematic and/or localized inflammation levels in various autoimmune, infectious, and nutritional inflammatory paradigms [25—28]. In particular, recent studies with $Na_v1.8$ ablated mice have shown that intact $Na_v1.8$ neurons are required to limit bacterial infections [29] and promote psoriasis-like inflammation [30]. Our own observations further suggest that $Na_v1.8$-expressing neurons are an important component of the regulation of diet-induced acute phase response.

4.1. $Na_v1.8$ neurons and energy balance

Peripheral nerves, largely made up of C-fibers, supply innervation to the entire gastrointestinal tract [31]. It has long been known that peripheral afferents innervating the gastrointestinal tract rapidly respond to a wide range of post-ingestive signals including but not limited to nutrients, gut peptides, and mechanical deformations [32—35]. Post-ingestive signals from the oral cavity and gastrointestinal tract provide the short-term feedback that controls feeding: for example, a subdiaphragmatic vagotomy disrupts food consumption [36]. However, the results of this procedure are difficult to interpret since vagotomized animals also exhibit impaired gastrointestinal motility. Selective surgical and capsaicin-induced deafferentation of the vagus nerve does produce a modest increase in meal size [37,38]. Likewise, mutant mice lacking gastric or intestinal vagal mechanoreceptors have increased meal frequency or duration without obesity [39,40]. Due to different methodological approaches (genetic, surgical, chemical) and targeted vagal populations, each of the prior studies on the manipulation of vagal afferents modifies meal patterning in different ways. However, they all agree on the fact that ablation of vagal afferents results neither in obesity nor in dramatic changes in food intake.

$Na_v1.8$ is present in a majority of vagal neurons [20,21]. Hence, $Na_v1.8$ neurons extensively innervate thoracic and abdominal viscera and their vasculature [20,21]. In line with the aforementioned literature, we demonstrated that $Na_v1.8$ neurons in the mouse are dispensable to the regulation of energy balance and feeding. The ablation of $Na_v1.8$ neurons only resulted in very modest meal patterning changes, including elevated feeding rate. Nonetheless, feeding rate is not considered an important determinant of daily food intake [41]. Furthermore, neuronal activation in the NTS caused by the ingestion of a large fatty meal was identical in ablated and control animals. Our results are consistent with those of other studies that reported unaltered c-Fos in the NTS of deafferented rats following gastric distention or cholecystokinin administration [42,43]. It is likely that circulating factors and the remaining fibers, e.g., those that do not express $Na_v1.8$, were sufficient to elicit neuronal activation in the dorsovagal complex. This interpretation is consistent with the increasingly accepted view of a high degree of convergence of post-ingestive signals at the levels of vagal afferents, including gastric mechanoreceptors as well as neurons in the nucleus of the solitary tract [33,43—45]. Based on observations that ablated mice do not normally respond to noxious stimuli or bacterial infections [15,29], $Na_v1.8$ neurons, including those in the vagus nerve, may be more important in regulating responses to noxious visceral stimuli rather than postprandial metabolic cues.

Of note, Voltage-gated sodium channels, such as $Na_v1.7$, are expressed in the brain including in neurons involved in energy balance [46]. One study reported widespread expression for $Na_v1.8$ in the mouse brain including the hypothalamus [47]. However, we have examined the brain of $Na_v1.8$-Cre-tdTomato reporter mice and found no evidence of any Cre activity in the hypothalamus (not shown). Instead, and in agreement with the Allen Brain Atlas (http://mouse.brain-map.org/experiment/show/69288285), we noticed sparse tdTomato-labeled cells in the cortex and basal forebrain. We cannot completely rule out that low levels of $Na_v1.8$-driven Cre activity in the forebrain may have contributed to phenotype observed in ablated animals. Future studies are thus warranted, for instance using brain-sparing technologies [48], to ablate $Na_v1.8$ neurons exclusively in the periphery.

4.2. Immunomodulatory functions of $Na_v1.8$ neurons in obesity

The ability of isolated sensory neurons to directly respond to saturated fatty acids has also been reported using electrophysiology and calcium signaling [49—51]. Obesity in humans has also been associated with elevated calcitonin gene-related peptide (CGRP), a neuropeptide deriving from subsets of C-fibers [52,53], indicating the stimulation of peripheral afferents in obesity. Nonetheless, the mechanisms linking afferent neurons to dietary-derived fat-induced inflammatory responses remain speculative. It is known that IL6 is a potent inducer of hepatic SAA1 [54,55], an acute phase response protein. Although dietary-derived saturated fatty acids can directly initiate the production of pro-inflammatory molecules from a variety of cell types [56—58], white adipose tissue is the most likely source of IL-6 in obesity. Indeed, IL-6 circulates at higher levels than other pro-inflammatory cytokines

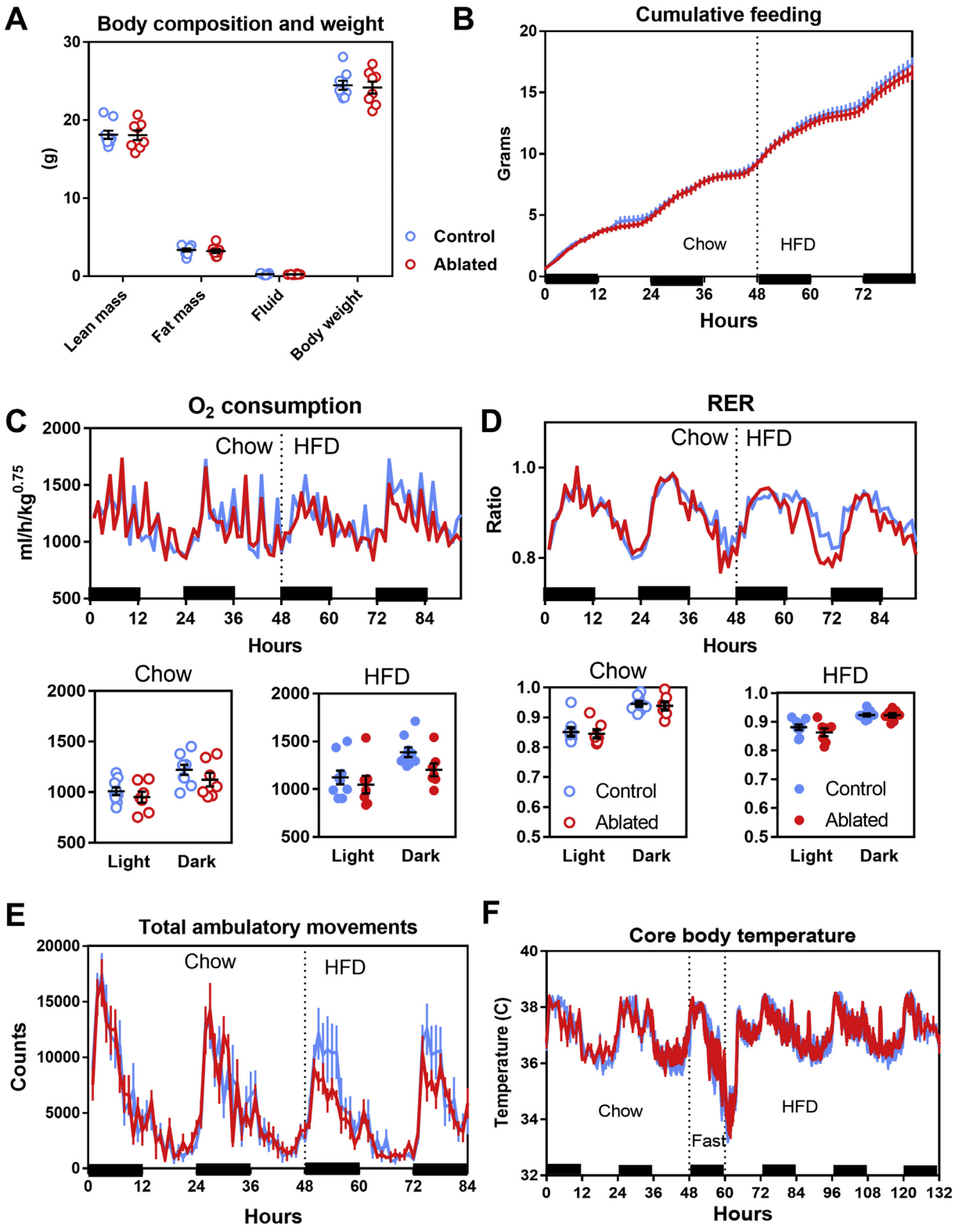

Figure 2: Metabolic characterization of ablated mice. (**A**) Body composition and body weight measured in age-matched animals were identical in control (blue) and ablated (red) mice fed on a chow diet, before entering TSE metabolic chambers (n = 7/group). (**B**) Cumulative food intake in metabolic chambers for control littermates (blue) and ablated mice (red bars). All mice were switched to a 42% high-fat diet at 48 h. (**C**–**D**) Respiratory exchange rate and oxygen consumption during the light and dark phase, before (open circles) and after high-fat diet exposure (filled circles). Metabolic rate parameters were identical in control (blue) and ablated (red) animals. (**E**) Total ambulatory movements (x, y, z directions) were not significantly different between genotypes. Nonetheless, we observed a trend towards lowered activity in ablated mice (red) after high-fat diet exposure. (**F**) Core body temperature monitored using telemetry demonstrated that ablated mice (red) normally regulated their temperature, even in response to dietary challenges including overnight fasting and high-fat diet exposure. In particular, fasting was associated with reduced core temperature in both groups. Conversely, temperature during the light phase was slightly raised in both groups after high-fat diet exposure (n = 6 control and n = 7 ablated).

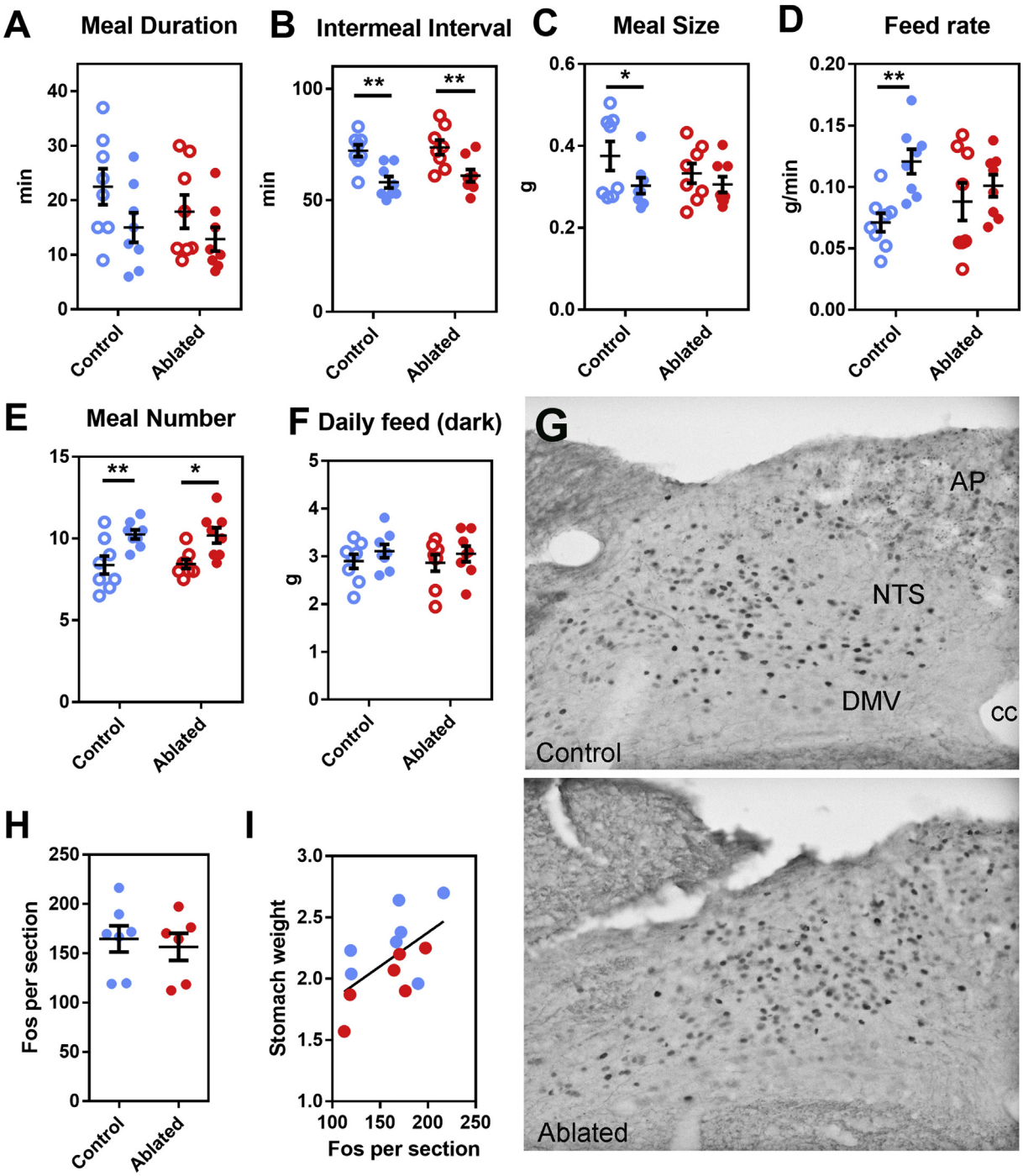

Figure 3: Characterization of meal patterns and postprandial neuronal activation. (**A**–**F**) Meal parameters of ablated (red) and controls (blue) measured in metabolic chambers during the dark phase (n = 7/group). Asterisks denote significant differences between chow- (open circles) and high-fat diet-fed mice (filled circles) (two-way ANOVA, with Bonferroni correction; *, $p < 0.05$; **, $p < 0.01$). (**G**) Immunohistochemistry for c-Fos in the dorsovagal complex of control (top image) and ablated mice (bottom image) 1 h 30 min after a large fatty meal. (**H, I**) The total number of c-Fos positive neurons in the dorsovagal complex per section was identical in both groups and positively correlated with the stomach weight (n = 7 control and n = 6 ablated). Error bars indicate SEM. Abbreviations: AP, area postrema; DMV, dorsal motor nucleus of the vagus nerve; cc, central canal; NTS, nucleus of the solitary tract.

in human obesity and is tightly correlated with the degree of adiposity and blood SAA1 [3–6]. In addition, high-fat diets stimulate the expression of adipose IL-6 and hepatic SAA1 [59], suggesting the existence of an IL-6-SAA1 axis stimulated by dietary fat. Our data show that the activity of $Na_v1.8$ neurons normally activates a compensatory response to inhibit the IL6-SAA1 axis upon chronic high-fat feeding or acute lard oil administration. In line with our findings, others have demonstrated that mice lacking the CGRP receptor show selectively elevated IL-6 in response to a post-fracture injury [60]. Therefore, it is likely that elevated adipose IL-6 in response to dietary fact is directly

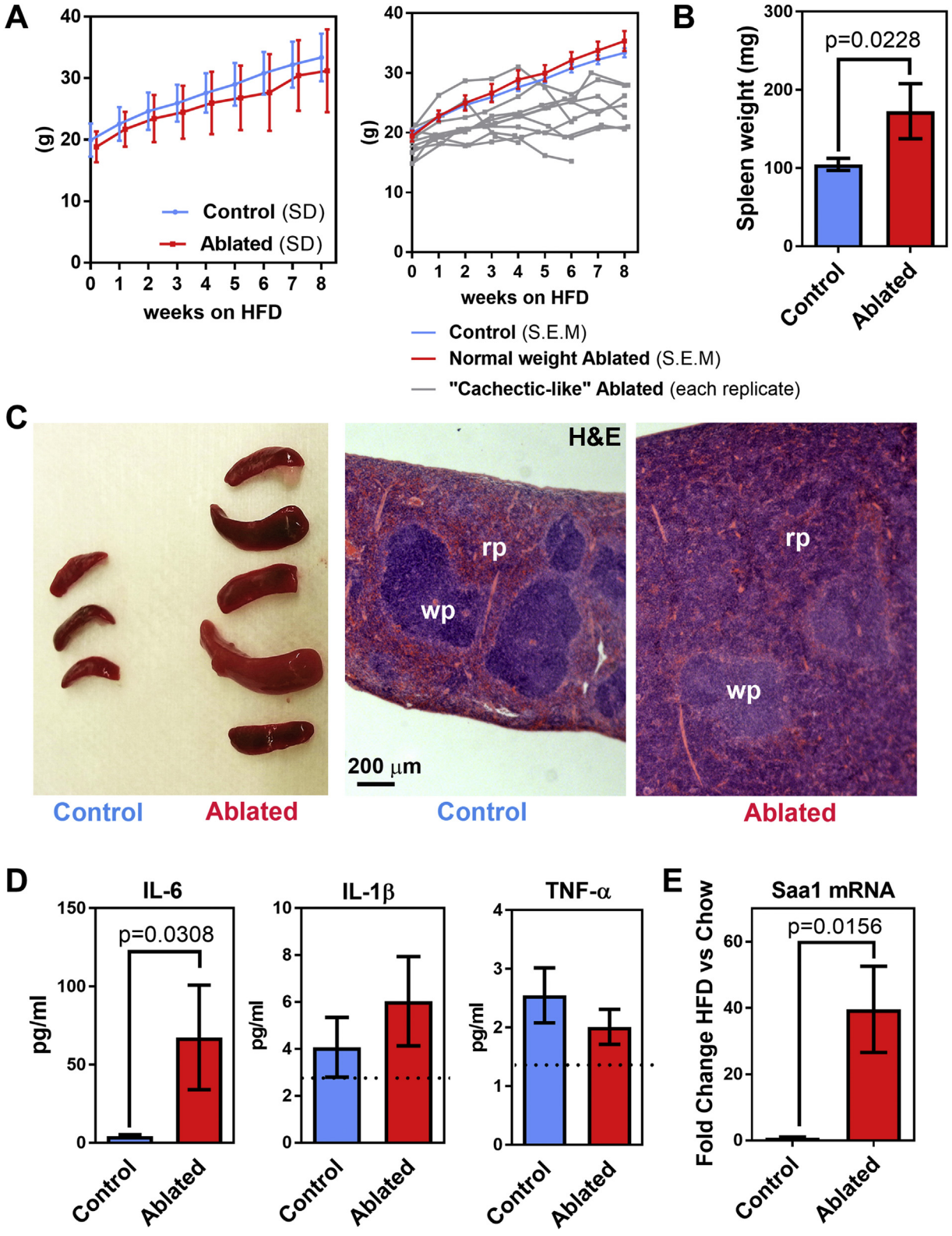

Figure 4: Ablated mice developed an acute phase response during chronic high-fat feeding. (**A**) Weekly weight gain was recorded after the start of the high-fat diet in control littermates (blue, n = 19) and ablated model mice (red, n = 21). Note that the error bars (left) indicating standard deviation is skewed toward the lowest values for the ablated group. Individual body weight curves indicate that a subset of ablated mice showed unexpected weight loss (gray lines). (**B**) Splenomegaly was observed in ablated mice after 9 weeks on the high-fat diet ($p < 0.05$, Student's t-test, unpaired). To varying degrees, the spleen of ablated mice was often visibly bigger than in control animals. (**C**) After 9 weeks on high-fat diet, the spleen of control littermates and ablated mice was stained with hematoxylin and eosin. In ablated mice with the most severe splenomegaly, both leukopenia and red pulp enlargement were evident. (**D**) Plasma levels of interleukin-6 (IL-6), IL-1β, and tumor necrosis alpha (TNF-α) measured after 9 weeks of high fat feeding ($p < 0.05$, Student's t-test, unpaired). The dotted line indicates the limit of detection (n = 12 controls and n = 8 ablated). (**E**) Expression of acute phase reactant Saa-1 in livers of ablated mice (red bars, n = 16) and their control littermates (blue bars, n = 24) ($p < 0.05$, Student's t-test, unpaired). Error bars indicate SEM.

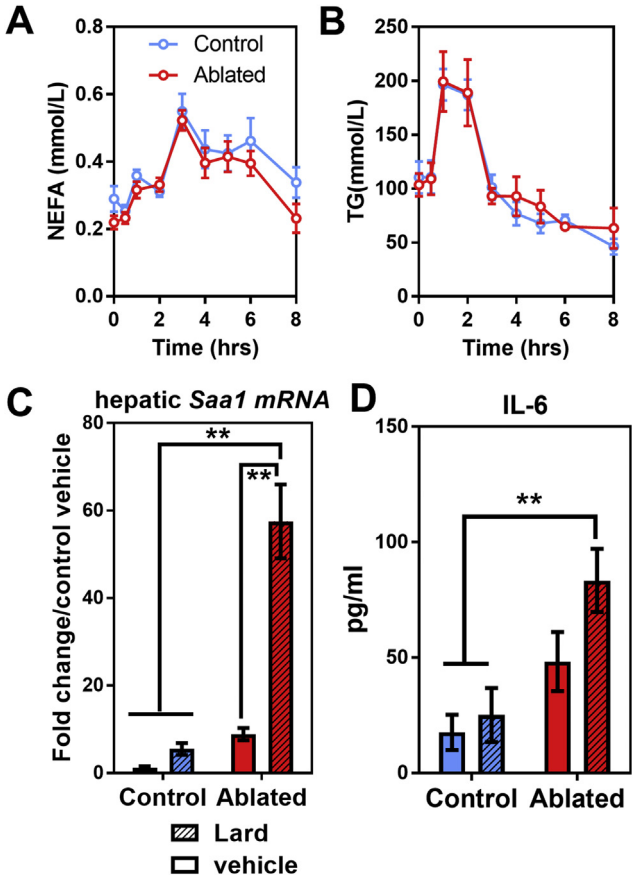

Figure 5: Saturated fat-induced cute phase response in ablated mice. (**A, B**) Plasma levels of triglyceride or non-esterified fatty acids after gavage of lard oil (open symbols) in control (blue) versus ablated animals (red). Kinetics of the appearance of triglycerides and non-esterified fatty acids in the blood stream after lard oil gavage is similar in both groups (n = 6/group). (**C**) Expression of Saa-1 mRNA in livers of lard-oil fed ablated mice (red bars; n = 10, saline group; n = 17 lard oil group) and their control littermates (white bars; n = 10, saline group; n = 11 lard oil group). (**D**) Plasma levels of IL-6 measured 3 h after lard oil or vehicle in ablated mice (red bars; n = 8, saline group; and n = 16, lard oil group) and their control littermates (white bars; n = 8, saline group; and n = 9, lard oil group). Asterisks denote significant differences when compared with littermate controls (two-way ANOVA, with Bonferroni correction; **, $p < 0.01$). Error bars indicate SEM.

linked to the absence of CGRP-producing C-fibers. Ablated mice fed on high-fat diet also showed splenic anomalies consistent with leukocytosis. Strikingly, IL-6 has been previously demonstrated to be required for leukocytosis (among other hematological anomalies) and hepatic SAA1 expression in response to chronic high-fat feeding in the mouse [59]. Thus, the splenic anomalies and elevated SAA1 seen in ablated mice are the direct result of chronically elevated IL-6.

4.3. Conclusions

Collectively, our experiments demonstrate that $Na_v1.8$ neurons are regulators of an IL-6-SAA1 axis in a diet-dependent manner. Understanding the links between obesity and acute phase reactants may help to combat comorbidities associated with diet-induced obesity. Modulating the activity of autonomic nerves by pharmacological or device-assisted (i.e., stimulator) means holds promise as a therapeutic approach for uncontrolled inflammatory states [61], and this study specifically suggests that stimulating visceral afferents could alleviate the obesity-associated acute phase response.

ACKNOWLEDGMENTS

We would like to thank Charlotte Lee, Danielle Lauzon, Ying Huang, Yang Liu, and Matthew Harper (UT Southwestern medical center) for their technical assistance. We are grateful to Dr. John Wood for providing us with $Na_v1.8$-Cre mice (6WIBR, University College London WC1E 6BT UK). We would like to thank the Mouse Metabolic Phenotyping Core at University of Texas Southwestern Medical Center at Dallas (supported by P01DK088761, PL1 DK081182, UL1RR024923). JKE supported by the NIH (P01DK088761; RL1DK081185). PES was supported by the NIH (R01-DK55758 and P01DK088761).

CONFLICT OF INTEREST

None declared.

APPENDIX A. SUPPLEMENTARY DATA

Supplementary data related to this article can be found at http://dx.doi.org/10.1016/j.molmet.2017.07.012.

REFERENCES

[1] Lumeng, C.N., Saltiel, A.R., 2011. Inflammatory links between obesity and metabolic disease. Journal of Clinical Investigation 121(6):2111–2117.
[2] Hotamisligil, G.S., 2006. Inflammation and metabolic disorders. Nature 444(7121):860–867.
[3] Roytblat, L., Rachinsky, M., Fisher, A., Greemberg, L., Shapira, Y., Douvdevani, A., et al., 2000. Raised interleukin-6 levels in obese patients. Obesity Research 8(9):673–675.
[4] Bastard, J.P., Jardel, C., Bruckert, E., Blondy, P., Capeau, J., Laville, M., et al., 2000. Elevated levels of interleukin 6 are reduced in serum and subcutaneous adipose tissue of obese women after weight loss. Journal of Clinical Endocrinology & Metabolism 85(9):3338–3342.
[5] Kern, P.A., Ranganathan, S., Li, C., Wood, L., Ranganathan, G., 2001. Adipose tissue tumor necrosis factor and interleukin-6 expression in human obesity and insulin resistance. American Journal of Physiology – Endocrinology and Metabolism 280(5):E745–E751.
[6] Sjoholm, K., Lundgren, M., Olsson, M., Eriksson, J.W., 2009. Association of serum amyloid A levels with adipocyte size and serum levels of adipokines: differences between men and women. Cytokine 48(3):260–266.
[7] Olefsky, J.M., Glass, C.K., 2010. Macrophages, inflammation, and insulin resistance. Annual Review of Physiology 72:219–246.
[8] Unger, R.H., Scherer, P.E., 2010. Gluttony, sloth and the metabolic syndrome: a roadmap to lipotoxicity. Trends in Endocrinology and Metabolism 21(6):345–352.
[9] Craig, A.D., 2002. How do you feel? Interoception: the sense of the physiological condition of the body. Nature Reviews Neuroscience 3(8):655–666.
[10] Moran, T.H., Ladenheim, E.E., Schwartz, G.J., 2001. Within-meal gut feedback signaling. International Journal of Obesity and Related Metabolic Disorders 25(Suppl. 5):S39–S41.
[11] Berthoud, H.R., Neuhuber, W.L., 2000. Functional and chemical anatomy of the afferent vagal system. Autonomic Neuroscience 85(1–3):1–17.
[12] Petho, G., Porszasz, R., Peitl, B., Szolcsanyi, J., 1999. Spike generation from dorsal roots and cutaneous afferents by hypoxia or hypercapnia in the rat in vivo. Experimental Physiology 84(1):1–15.
[13] Goehler, L.E., Gaykema, R.P., Hansen, M.K., Anderson, K., Maier, S.F., Watkins, L.R., 2000. Vagal immune-to-brain communication: a visceral chemosensory pathway. Autonomic Neuroscience 85(1–3):49–59.
[14] Julius, D., Basbaum, A.I., 2001. Molecular mechanisms of nociception. Nature 413(6852):203–210.

[15] Abrahamsen, B., Zhao, J., Asante, C.O., Cendan, C.M., Marsh, S., Martinez-Barbera, J.P., et al., 2008. The cell and molecular basis of mechanical, cold, and inflammatory pain. Science 321(5889):702–705.
[16] Stirling, L.C., Forlani, G., Baker, M.D., Wood, J.N., Matthews, E.A., Dickenson, A.H., et al., 2005. Nociceptor-specific gene deletion using heterozygous NaV1.8-Cre recombinase mice. Pain 113(1–2):27–36.
[17] Dib-Hajj, S.D., Cummins, T.R., Black, J.A., Waxman, S.G., 2010. Sodium channels in normal and pathological pain. Annual Review of Neuroscience 33:325–347.
[18] Djouhri, L., Fang, X., Okuse, K., Wood, J.N., Berry, C.M., Lawson, S.N., 2003. The TTX-resistant sodium channel Nav1.8 (SNS/PN3): expression and correlation with membrane properties in rat nociceptive primary afferent neurons. Journal of Physiology 550(Pt 3):739–752.
[19] Fukuoka, T., Kobayashi, K., Yamanaka, H., Obata, K., Dai, Y., Noguchi, K., 2008. Comparative study of the distribution of the alpha-subunits of voltage-gated sodium channels in normal and axotomized rat dorsal root ganglion neurons. Journal of Comparative Neurology 510(2):188–206.
[20] Gautron, L., Sakata, I., Udit, S., Zigman, J.M., Wood, J.N., Elmquist, J.K., 2011. Genetic tracing of Nav1.8-expressing vagal afferents in the mouse. Journal of Comparative Neurology 519(15):3085–3101.
[21] Yuan, X., Huang, Y., Shah, S., Wu, H., Gautron, L., 2016. Levels of cocaine- and amphetamine-regulated transcript in vagal afferents in the mouse are unaltered in response to metabolic challenges. eNeuro 3(5).
[22] Gautron, L., Lee, C.E., Lee, S., Elmquist, J.K., 2012. Melanocortin-4 receptor expression in different classes of spinal and vagal primary afferent neurons in the mouse. Journal of Comparative Neurology 520(17):3933–3948.
[23] Bookout, A.L., Jeong, Y., Downes, M., Yu, R.T., Evans, R.M., Mangelsdorf, D.J., 2006. Anatomical profiling of nuclear receptor expression reveals a hierarchical transcriptional network. Cell 126(4):789–799.
[24] Fox, E.A., Biddinger, J.E., Jones, K.R., McAdams, J., Worman, A., 2013. Mechanism of hyperphagia contributing to obesity in brain-derived neurotrophic factor knockout mice. Neuroscience 229:176–199.
[25] Razavi, R., Chan, Y., Afifiyan, F.N., Liu, X.J., Wan, X., Yantha, J., et al., 2006. TRPV1+ sensory neurons control beta cell stress and islet inflammation in autoimmune diabetes. Cell 127(6):1123–1135.
[26] Luyer, M.D., Greve, J.W., Hadfoune, M., Jacobs, J.A., Dejong, C.H., Buurman, W.A., 2005. Nutritional stimulation of cholecystokinin receptors inhibits inflammation via the vagus nerve. Journal of Experimental Medicine 202(8):1023–1029.
[27] Long, N.C., Frevert, C.W., Shore, S.A., 1996. Role of C fibers in the inflammatory response to intratracheal lipopolysaccharide. American Journal of Physiology 271(3 Pt 1):L425–L431.
[28] Levine, J.D., Dardick, S.J., Roizen, M.F., Helms, C., Basbaum, A.I., 1986. Contribution of sensory afferents and sympathetic efferents to joint injury in experimental arthritis. Journal of Neuroscience 6(12):3423–3429.
[29] Chiu, I.M., Heesters, B.A., Ghasemlou, N., Von Hehn, C.A., Zhao, F., Tran, J., et al., 2013. Bacteria activate sensory neurons that modulate pain and inflammation. Nature 501(7465):52–57.
[30] Riol-Blanco, L., Ordovas-Montanes, J., Perro, M., Naval, E., Thiriot, A., Alvarez, D., et al., 2014. Nociceptive sensory neurons drive interleukin-23-mediated psoriasiform skin inflammation. Nature 510(7503):157–161.
[31] Prechtl, J.C., Powley, T.L., 1990. The fiber composition of the abdominal vagus of the rat. Anatomy and Embryology (Berlin) 181(2):101–115.
[32] Iggo, A., 1957. Gastric mucosal chemoreceptors with vagal afferent fibres in the cat. Quarterly Journal of Experimental Physiology & Cognate Medical Sciences 42(4):398–409.
[33] Williams, E.K., Chang, R.B., Strochlic, D.E., Umans, B.D., Lowell, B.B., Liberles, S.D., 2016. Sensory neurons that detect stretch and nutrients in the digestive system. Cell.
[34] Blackshaw, L.A., Grundy, D., 1990. Effects of cholecystokinin (CCK-8) on two classes of gastroduodenal vagal afferent fibre. Journal of the Autonomic Nervous System 31(3):191–201.
[35] Hillsley, K., Grundy, D., 1998. Serotonin and cholecystokinin activate different populations of rat mesenteric vagal afferents. Neuroscience Letters 255(2):63–66.
[36] Powley, T.L., Chi, M.M., Baronowsky, E.A., Phillips, R.J., 2005. Gastrointestinal tract innervation of the mouse: afferent regeneration and meal patterning after vagotomy. American Journal of Physiology – Regulatory, Integrative and Comparative Physiology 289(2):R563–R574.
[37] Schwartz, G.J., Salorio, C.F., Skoglund, C., Moran, T.H., 1999. Gut vagal afferent lesions increase meal size but do not block gastric preload-induced feeding suppression. American Journal of Physiology 276(6 Pt 2):R1623–R1629.
[38] Chavez, M., Kelly, L., York, D.A., Berthoud, H.R., 1997. Chemical lesion of visceral afferents causes transient overconsumption of unfamiliar high-fat diets in rats. American Journal of Physiology 272(5 Pt 2):R1657–R1663.
[39] Fox, E.A., Phillips, R.J., Baronowsky, E.A., Byerly, M.S., Jones, S., Powley, T.L., 2001. Neurotrophin-4 deficient mice have a loss of vagal intraganglionic mechanoreceptors from the small intestine and a disruption of short-term satiety. Journal of Neuroscience 21(21):8602–8615.
[40] Fox, E.A., Phillips, R.J., Martinson, F.A., Baronowsky, E.A., Powley, T.L., 2001. C-Kit mutant mice have a selective loss of vagal intramuscular mechanoreceptors in the forestomach. Anatomy and Embryology (Berlin) 204(1):11–26.
[41] Sclafani, A., 1994. Eating rates in normal and hypothalamic hyperphagic rats. Physiology & Behavior 55(3):489–494.
[42] Berthoud, H.R., Patterson, L.M., Willing, A.E., Mueller, K., Neuhuber, W.L., 1997. Capsaicin-resistant vagal afferent fibers in the rat gastrointestinal tract: anatomical identification and functional integrity. Brain Research 746(1–2):195–206.
[43] Baptista, V., Browning, K.N., Travagli, R.A., 2007. Effects of cholecystokinin-8s in the nucleus tractus solitarius of vagally deafferented rats. American Journal of Physiology – Regulatory, Integrative and Comparative Physiology 292(3):R1092–R1100.
[44] Appia, F., Ewart, W.R., Pittam, B.S., Wingate, D.L., 1986. Convergence of sensory information from abdominal viscera in the rat brain stem. American Journal of Physiology 251(2 Pt 1):G169–G175.
[45] Schwartz, G.J., Moran, T.H., 1996. Sub-diaphragmatic vagal afferent integration of meal-related gastrointestinal signals. Neuroscience and Biobehavioral Reviews 20(1):47–56.
[46] Branco, T., Tozer, A., Magnus, C.J., Sugino, K., Tanaka, S., Lee, A.K., et al., 2016. Near-perfect synaptic integration by Nav1.7 in hypothalamic neurons regulates body weight. Cell 165(7):1749–1761.
[47] Lu, V.B., Ikeda, S.R., Puhl 3rd, H.L., 2015. A 3.7 kb fragment of the mouse Scn10a gene promoter directs neural crest but not placodal lineage EGFP expression in a transgenic animal. Journal of Neuroscience 35(20):8021–8034.
[48] Pereira, M.M.A., Mahu, I., Seixas, E., Martinez-Sanchez, N., Kubasova, N., Pirzgalska, R.M., et al., 2017. Corrigendum: a brain-sparing diphtheria toxin for chemical genetic ablation of peripheral cell lineages. Nature Communications 8:15673.
[49] Ochoa-Cortes, F., Ramos-Lomas, T., Miranda-Morales, M., Spreadbury, I., Ibeakanma, C., Barajas-Lopez, C., et al., 2010. Bacterial cell products signal to mouse colonic nociceptive dorsal root ganglia neurons. American Journal of Physiology – Gastrointestinal and Liver Physiology 299(3):G723–G732.
[50] Barajon, I., Serrao, G., Arnaboldi, F., Opizzi, E., Ripamonti, G., Balsari, A., et al., 2009. Toll-like receptors 3, 4, and 7 are expressed in the enteric nervous system and dorsal root ganglia. The Journal of Histochemistry and Cytochemistry: Official Journal of the Histochemistry Society 57(11):1013–1023.
[51] Randich, A., Tyler, W.J., Cox, J.E., Meller, S.T., Kelm, G.R., Bharaj, S.S., 2000. Responses of celiac and cervical vagal afferents to infusions of lipids in the jejunum or ileum of the rat. American Journal of Physiology – Regulatory, Integrative and Comparative Physiology 278(1):R34–R43.

[52] Zelissen, P.M., Koppeschaar, H.P., Lips, C.J., Hackeng, W.H., 1991. Calcitonin gene-related peptide in human obesity. Peptides 12(4):861—863.

[53] Gram, D.X., Hansen, A.J., Wilken, M., Elm, T., Svendsen, O., Carr, R.D., et al., 2005. Plasma calcitonin gene-related peptide is increased prior to obesity, and sensory nerve desensitization by capsaicin improves oral glucose tolerance in obese Zucker rats. European Journal of Endocrinology/European Federation of Endocrine Societies 153(6):963—969.

[54] Matsui, S., Yamane, T., Kobayashi-Hattori, K., Oishi, Y., 2013. Calcitonin gene-related peptide upregulates serum amyloid A synthesis through activation of interleukin-6. Bioscience, Biotechnology, and Biochemistry 77(10): 2151—2153.

[55] Fattori, E., Cappelletti, M., Costa, P., Sellitto, C., Cantoni, L., Carelli, M., et al., 1994. Defective inflammatory response in interleukin 6-deficient mice. Journal of Experimental Medicine 180(4):1243—1250.

[56] Weigert, C., Brodbeck, K., Staiger, H., Kausch, C., Machicao, F., Haring, H.U., et al., 2004. Palmitate, but not unsaturated fatty acids, induces the expression of interleukin-6 in human myotubes through proteasome-dependent activation of nuclear factor-kappaB. Journal of Biological Chemistry 279(23): 23942—23952.

[57] Jia, L., Vianna, C.R., Fukuda, M., Berglund, E.D., Liu, C., Tao, C., et al., 2014. Hepatocyte Toll-like receptor 4 regulates obesity-induced inflammation and insulin resistance. Nature Communications 5:3878.

[58] Ajuwon, K.M., Spurlock, M.E., 2005. Palmitate activates the NF-kappaB transcription factor and induces IL-6 and TNFalpha expression in 3T3-L1 adipocytes. The Journal of Nutrition 135(8):1841—1846.

[59] Pini, M., Rhodes, D.H., Fantuzzi, G., 2011. Hematological and acute-phase responses to diet-induced obesity in IL-6 KO mice. Cytokine 56(3): 708—716.

[60] Guo, T.Z., Wei, T., Shi, X., Li, W.W., Hou, S., Wang, L., et al., 2012. Neuropeptide deficient mice have attenuated nociceptive, vascular, and inflammatory changes in a tibia fracture model of complex regional pain syndrome. Molecular Pain 8:85.

[61] Andersson, U., Tracey, K.J., 2011. Reflex principles of immunological homeostasis. Annual Review of Immunology.

